Thermochimica Acta, 223 (1993) 7–22
Elsevier Science Publishers B.V., Amsterdam

Development of a high-temperature differential scanning calorimeter equipped with a triple-cell system

Yoichi Takahashi * and Masami Asou

Department of Nuclear Engineering, University of Tokyo, Hongo, Bunkyo-ku, Tokyo 113 (Japan)

(Received 28 January 1993; accepted 28 January 1993)

Abstract

A new differential scanning calorimeter (DSC) for heat capacity measurements up to 1500 K has been developed. In order to overcome difficulties encountered in high-temperature heat capacity measurements with conventional DSC equipment, two new concepts were adopted for the design of this apparatus: a "triple-cell" system and triple-adiabatic temperature control. The heat capacities of Mo, Pt and UO_2 were determined from 300 to 1500 K to test the new apparatus. The heat capacities of Ni and Ti, which are known to have phase transitions at 631 K and at around 1160 K, respectively, were also measured. The precision of the apparatus was estimated to be within ±3%. A comparison of the results obtained by two analytical methods, the enthalpy method and the scanning method, is also made.

INTRODUCTION

Differential scanning calorimetry (DSC) has been used to study the thermal behavior of materials and to determine their heat capacities. The temperature range of the heat capacity measurements, however, has as far been usually limited to below 1000 K. The main reason for this limitation is ascribed to the fact that radiation heat-loss increases with temperature and, as a result, the thermal stability and repeatability of the isothermal baseline signals become poor. For precise heat capacity measurements at high temperatures, it is thus necessary to stabilize the temperature control and establish the isothermal baseline.

The aim of the present study is to develop a new type of DSC, which can determine, easily and precisely, heat capacity values up to 1500 K. The heat capacities of Mo, Pt, UO_2, Ni and Ti were determined using this DSC, in order to check the precision and reliability of the new apparatus.

* Corresponding author.

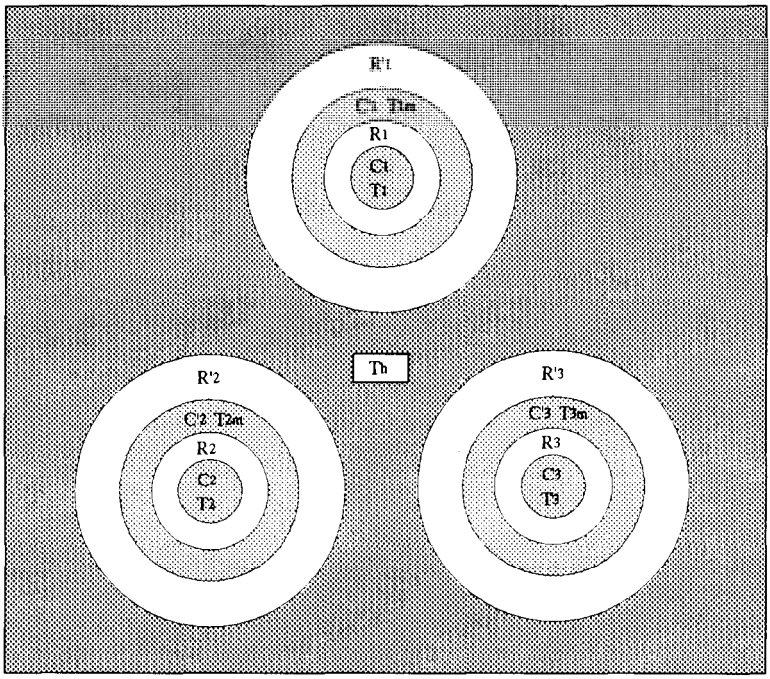

Fig. 1. Conceptual diagram of the "triple-cell" DSC. T_1, T_2, T_3, temperature of the sample; T_{1m}, T_{2m}, T_{3m}, temperature of the holder where the thermocouple wire is anchored; T_h, temperature of the isothermal plate; C_1, C_2, C_3, heat capacity of the sample; C_{1m}, C_{2m}, C_{3m}, heat capacity of the holder; R_1, R_2, R_3, thermal resistance between the holder and the sample; R_1', R_2', R_3', thermal resistance between the holder and the isothermal plate; Subscripts: 1, empty side; 2, reference side; 3, sample side.

DEVELOPMENT OF THE NEW DSC APPARATUS

The principle of the triple-cell system

In order to obtain precise heat capacity measurements at high temperatures, we adopted the new "triple-cell" concept, first described by Wunderlich [1]. The principle of the triple-cell system is briefly summarized as follows.

The conceptual construction of the new DSC is illustrated in Fig. 1. The fundamental thermal equations for this system are given by eqns. (1)–(3)

$$\frac{1}{R_1'}(T_h - T_{1m}) = C_{1m}\frac{dT_{1m}}{dt} + C_1\frac{dT_1}{dt} \quad (1)$$

$$\frac{1}{R_2'}(T_h - T_{2m}) = C_{2m}\frac{dT_{2m}}{dt} + C_2\frac{dT_2}{dt} \quad (2)$$

$$\frac{1}{R_3'}(T_h - T_{3m}) = C_{3m}\frac{dT_{3m}}{dt} + C_3\frac{dT_3}{dt} \quad (3)$$

where the subscripts $i = 1$–3 indicate the empty side, reference side and

sample side, respectively, T_i is the temperature of the sample, T_h the temperature of the isothermal plate, T_{im} the temperature of the sample-pan holder, R_i' the thermal resistance between the holder and the isothermal plate, C_{im} the heat capacity of the holder, and C_i the heat capacity of the sample. Suppose an empty sample pan is placed on the empty side, a pan filled with the reference material on the reference side and a pan filled with the sample on the sample side, and these three sample pans are then heated from the heat source (isothermal plate) through the thermal resistances R and R'.

Assuming that $R_i \leq R_i'$, $R_1' = R_2' = R_3'$ and the heating rate is equal to dT_h/dt everywhere on the isothermal plate during a scan, we can obtain the heat capacity of the sample C_s from only a single run using the equation

$$C_s = C_r \frac{T_{1m} - T_{3m}}{T_{1m} - T_{2m}} \tag{4}$$

where C_r is the heat capacity of the reference material, and $(T_{1m} - T_{3m})$ and $(T_{1m} - T_{2m})$ are the observed temperature differences between the sample and the empty pan, and between the reference and the empty pan, respectively. Thus, this measuring system eliminates the necessity for the three separate runs in conventional twin-cell systems.

Even when the condition of $R_1' = R_2' = R_3'$ fails, only two separate runs are needed in this system. The first run is carried out with three empty sample pans on all sides; this run will be referred to as the "blank (all-empty-pans)" run. The temperature differences observed in this case are given by

$$\Delta T_{2m}^{B} = (T_{2m} - T_{1m})^{B} = \left(1 - \frac{R_2'}{R_1'}\right)(T_h - T_{1m}) \tag{5}$$

$$\Delta T_{3m}^{B} = (T_{3m} - T_{1m})^{B} = \left(1 - \frac{R_3'}{R_1'}\right)(T_h - T_{1m}) \tag{6}$$

where the superscript B indicates the result of a "blank run".

The second run is then performed with the empty pan on the empty side (1), the pan filled with reference material on the reference side (2) and the pan filled with sample on the sample side (3). The temperature differences are represented by

$$\Delta T_{2m} = (T_{2m} - T_{1m}) = \left(1 - \frac{R_2'}{R_1'}\right)(T_h - T_{1m}) - R_2'(C_2 - C_1)\frac{dT}{dt} \tag{7}$$

$$\Delta T_{3m} = (T_{3m} - T_{1m}) = \left(1 - \frac{R_3'}{R_1'}\right)(T_h - T_{1m}) - R_3'(C_3 - C_1)\frac{dT}{dt} \tag{8}$$

By subtracting eqns. (5) and (6) from eqns. (7) and (8), respectively, we

obtain

$$\Delta T_{3m} - \Delta T^{B}_{3m} = -R'_3(C_3 - C_1)\frac{dT}{dt} \tag{9}$$

$$\Delta T_{2m} - \Delta T^{B}_{2m} = -R'_2(C_2 - C_1)\frac{dT}{dt} \tag{10}$$

C_s is thus given by

$$C_s = C_r \frac{R'_2 \Delta T_{3m} - \Delta T^{B}_{3m}}{R'_3 \Delta T_{2m} - \Delta T^{B}_{2m}} \tag{11}$$

Therefore, knowing the value of R'_2/R'_3, C_s can be determined from two separate runs, including the blank run. The descriptions above refer to the principle of the scanning method; it also applies to the enthalpy method.

Experimental set-up of the apparatus

Sample section and cells

Schematic diagrams of the sample section are shown in Fig. 2. The top view shows the location of the cells for the sample, the reference and the empty sides. Each cell has a sample-pan holder, made of Pt–13%Rh flat plates 0.3 mm thick, which is connected by three bridges (0.3 mm in width) to the isothermal plate, in order to avoid the effect of cross-flow between the cells and to provide adequate thermal resistance for detection. The isothermal plate is made of Pt–13%Rh alloy, and is set in an isothermal container made of Pt–10%Rh alloy. A sample pan with a lid, made of Pt–10%Rh alloy, is also shown in Fig. 2.

Adiabatic control

The experimental set-up of the new DSC apparatus is shown in Fig. 3. When measuring precise heat capacities at high temperatures, sufficient temperature control is most important. We therefore adopted the triple-adiabatic temperature control system to attain thermal stability in the calorimeter, even above 1000 K. A block diagram of the triple-adiabatic temperature control system is shown in Fig. 4. The sample section is surrounded by three adiabatic walls. The walls are made of AlN, which has a better thermal conductivity than Al_2O_3 or BN, by a factor of 2–3 at high temperatures. Platinum foils are put inside the walls in order to minimize radiation heat-loss. The innermost adiabatic wall is divided into upper and lower sections, each of which can be controlled separately to eliminate the effect of convection of inert gas. They are further surrounded by double adiabatic walls, and the thermal stability is secured by all of these adiabatic

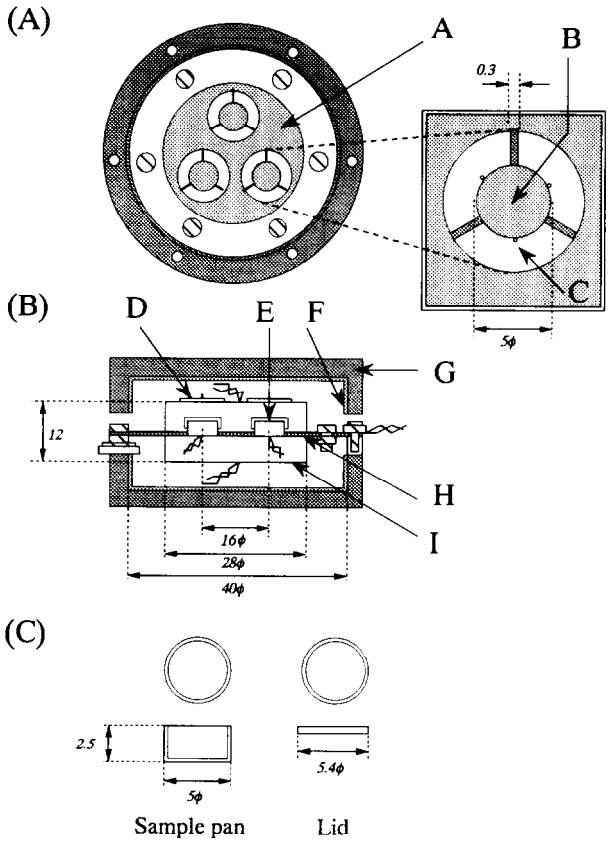

Fig. 2. Schematics of the sample section. A, isothermal plate; B, sample holder; C, pin for holding sample cell; D, lid; E, sample cell; F, platinum foil; G, adiabatic wall; H, isothermal plate; I, isothermal container.

walls. It is considered that the temperature fluctuations in the sample section are within about ±0.1 K during measurement.

Temperature sensing system

A block diagram of the temperature sensing system is shown in Fig. 5. R-type thermocouples, 0.3 mm in diameter, are used for detecting temperature differences. The Pt-wires are connected to the rear surface of the sample holders of the three cells, and the isothermal plate made of Pt-13%Rh alloy acts as another contact for the wires of the thermocouples. The output signals of temperature differences between the empty side and the reference side and between the empty side and the sample side, are detected by these thermocouples with the Pt-wire connected to the sample side and a Pt–13%Rh wire connected to the center of the isothermal plate.

The thermocouple for measuring the sample temperature was calibrated using pure metals (Sn, Ag).

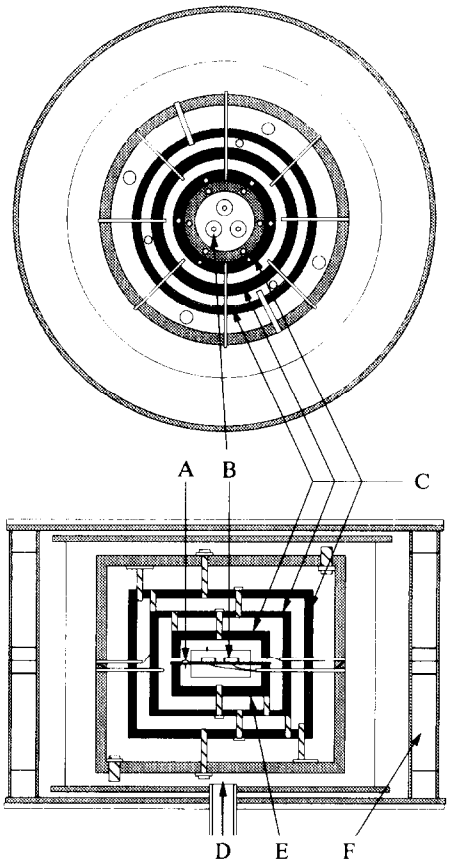

Fig. 3. Schematic view of the new DSC apparatus. A, thermocouple for program control; B, sample cell; C, adiabatic heater wall; D, Ar gas; E, program control heater wall; F, coolant.

Analytical procedure for heat capacity measurement

For heat capacity measurements, two different methods, a scanning method and an enthalpy method, were used in this study.

The "scanning method" refers to heat capacity measurements in which the output signals are continuously converted to heat capacity values over the range of the temperature scan. For a given temperature range of a scan, the quantities required that must be recorded are the differences in ordinate displacement between the reference and the blank, and between the sample and the blank, because these are proportional to the heat capacities of the reference material and sample, respectively.

However, the initial isothermal baseline of the sample run is not always the same as that of a blank run, and thus it is necessary to adjust each baseline. In this study, we adjusted it as shown in Fig. 6. The actual procedures are as follows. First, we displace the baseline of the sample run

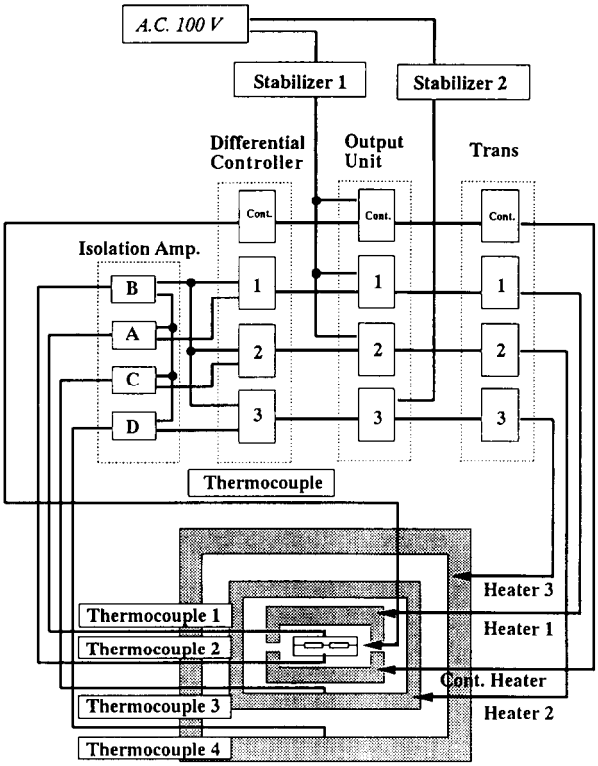

Fig. 4. Block diagram of the triple-adiabatic temperature control system.

so as to overlap it with that of the blank run (A)→(B). Next, the final isothermal baseline of the sample run is shifted so as to fit with that of the blank run (B)→(C). Then the difference between the outputs of the sample run and of the blank run is calculated over a steady state temperature region (C). The corresponding values for the reference material are calculated in a similar manner. The heat capacity of the sample

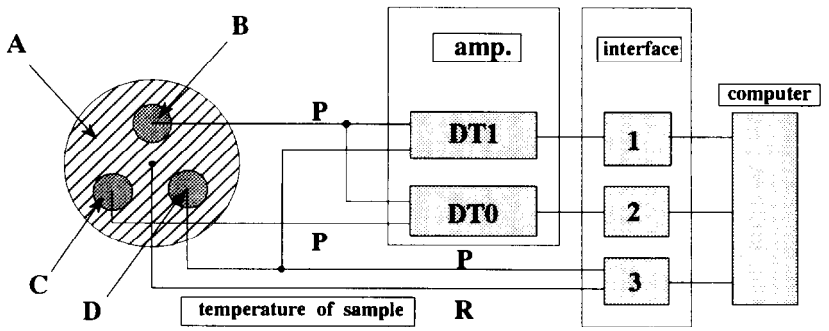

Fig. 5. Block diagram of the temperature-sensing system. A, isothermal plate; B, empty side; C, reference side; D, sample side.

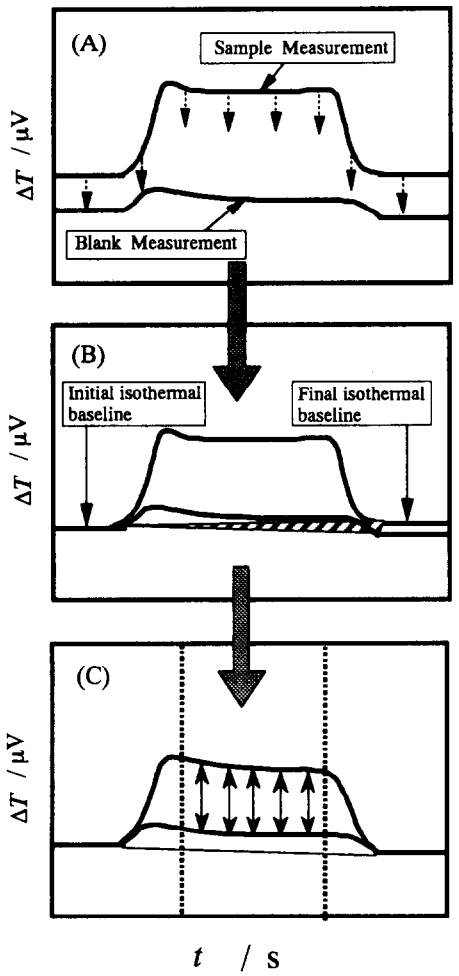

Fig. 6. Schematic of the procedure for the scanning method.

is then determined by comparing the two values obtained for the sample and the reference material.

The "enthalpy method" refers to heat capacity measurements in which all the output signals during a temperature scan are integrated to give the total enthalpy change (ΔH) for the given temperature interval (ΔT). The quantity $\Delta H/\Delta T$ is taken as the value of the heat capacity at the midpoint of the temperature interval. The sequence of enthalpy runs is shown schematically in Fig. 7. The initial isothermal baseline value is recorded, and the first scan is initiated. The output signals are recorded during a scan, including those during transitions, until it reaches the preset temperature, when the final baseline is recorded. The isothermal baselines at the initial and final temperatures are interpolated linearly to give the postlated baseline for temperatures within the interval. The integrated values of

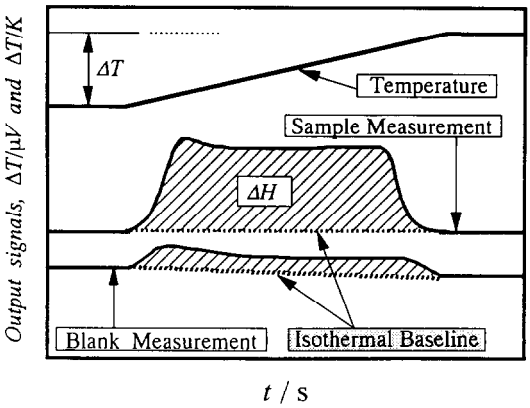

Fig. 7. Schematic of the procedure for the enthalpy method.

output signals during the scan are then calculated, taking into account the interpolated baseline, as shown in Fig. 7. This procedure is performed on the measurements of the sample, the reference and on the blank runs. The heat change for the sample is thus calculated by subtracting the area for the blank run from that for the sample run, and the heat capacity of the sample is determined by comparing the heat change for the sample with that for the reference material, taking into account the calibration constant.

CALIBRATION OF THE APPARATUS AND RESULTS OF HEAT CAPACITY MEASUREMENTS

Materials

Two pieces of NBS α-Al_2O_3 calorimetric standard (SRM-720) were used for determining the calibration constant.

The molybdenum and nickel sample pellets used for the heat capacity measurements were from Johnson Matthey, Materials Technology, Co. The platinum sample was provided by Shinku-Riko Co. The titanium sample was purchased from Furuuchi-Kagaku Co. The UO_2 sample pellet was provided by the Nippon Nuclear Fuel Development Co., Ltd. The masses and purities of the samples are listed in Table 1.

Calibration of the sample temperature

The sample temperature sensed by an R-type thermocouple was calibrated using the melting points of pure metals (Sn, Ag). The melting temperatures observed for Sn and Ag were 504.55 K (±0.3 K) and 1234.75 K (±0.3 K), respectively, and were consistent with the values of ITS-90 (505.078 K and 1234.75 K) within the detectable sensitivity of the apparatus.

TABLE 1

Masses and purities of the samples

Sample	Mass of sample/mg	Purity/%	O/M
α-Al_2O_3	40.96	99.99	
(SRM-720)	37.76	99.99	
Pt	286.53	99.99	
Mo	125.63	99.99	
UO_2	132.19	99.8	2.000
Ni	101.64	99.995	
	150.76	99.995	
Ti	61.72	99.9	

Determination of the calibration constant

The apparatus was calibrated, prior to the measurements, using the NBS reference material α-Al_2O_3. In the calibration, the enthalpy method was used, in which the total enthalpy change of the sample over a 25 K interval was measured with a scanning rate of 5 K min^{-1}. In order to check the difference in sensitivity between the sample side and the reference side, two α-Al_2O_3 samples were placed on the sample side and the reference side, with the empty pan on the empty side, and the calibration constant ($k = R_2'/R_3'$) was determined over the range 300–1500 K. The results are shown in Fig. 8. It can be seen that the calibration constant is roughly equal

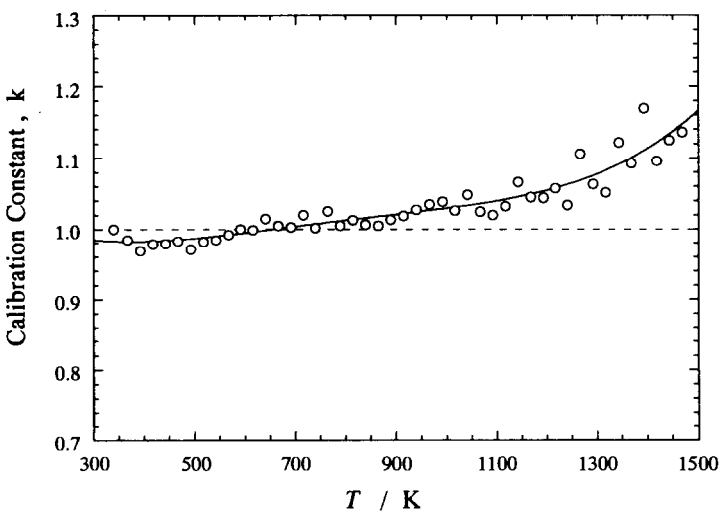

Fig. 8. Calibration constant k for heat capacity measurements. ○, experimental values; ——, polynomial expression.

to unity below 1000 K, but it deviates slowly from unity above 1000 K with increasing temperature. This may be attributed to the change in heat transfer from conduction through the isothermal plate to radiation. The calibration constant was determined as a function of temperature using the least-squares method. The deviation of the data from the fitting curve increases slightly at high temperatures because of the increasing difficulties of temperature control. The experimental uncertainty of this apparatus was considered to be within ±1–2% below 1000 K, and ±2–3% above this temperature.

Heat capacity measurements on Pt, Mo and UO_2

The heat capacity of Pt was determined using the enthalpy method from 300 to 1500 K. The results are shown in Fig. 9. The two series of experimenal results are consistent, within the estimated experimental uncertainty, although the results of the second run were slightly lower, by about 1%. The present results also agree well with the literature values [2, 3]. The repeatability of the data was considered to be ±2–3% over the temperature range of the measurements.

The heat capacity of Mo determined from 300 to 1500 K is shown in Fig. 10. The results are consistent with the literature values [4], within the estimated experimental uncertainty (±3%), indicating the high reliability of the new DSC apparatus.

Figure 11(a) shows the results of heat capacity measurements on UO_2 from 300 to 1500 K; they agree well with the literature values [5], although

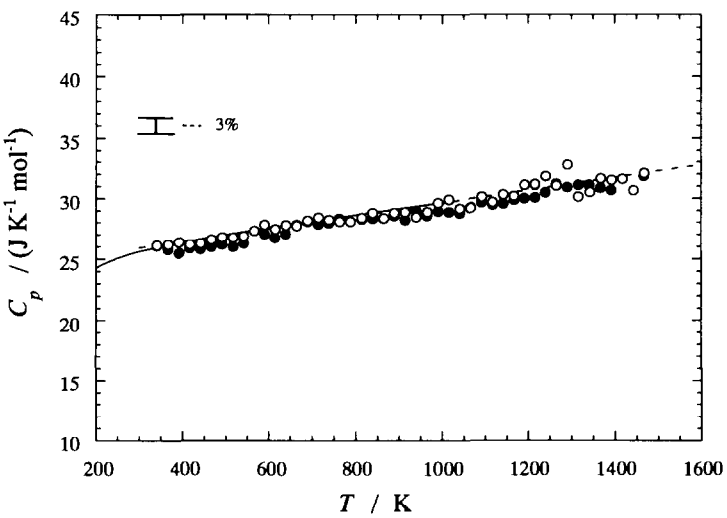

Fig. 9. Heat capacity of Pt. ○, ●, runs 1 and 2 (present work); – – –, Hultgren et al. [2]; ——, Yokokawa and Takahashi [3].

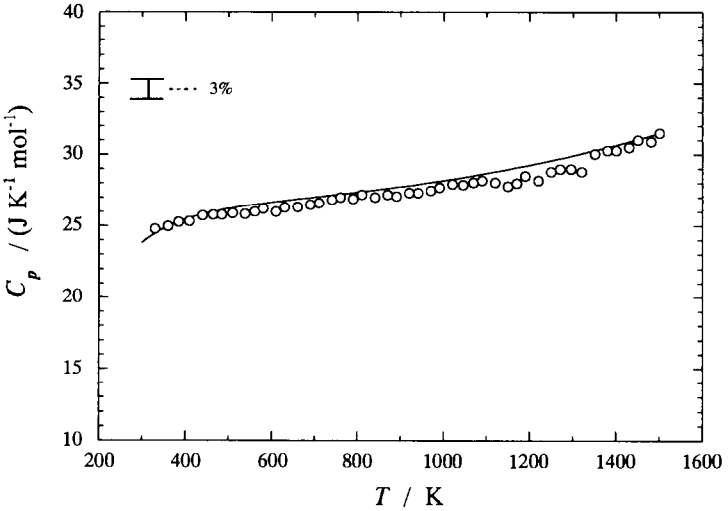

Fig. 10. Heat capacity of Mo. O, present work; ——, Ditmars et al. [4].

our values are slightly lower, by about 2%. The repeatability of the values was considered to be ±2–3% over the temperature range of the measurements. This indicates that the heat capacity can be determined precisely (±2–3%), even for a sample of low thermal conductivity.

A comparison of the enthalpy and scanning methods

The heat capacity of UO_2 was also calculated using the scanning method in order to compare this data with those obtained using the enthalpy method. In this study, we determined only one heat capacity value during a scan of 25 K at a temperature at which a steady state had been reached. The results are shown in Fig. 11(b); they are very close to those obtained using

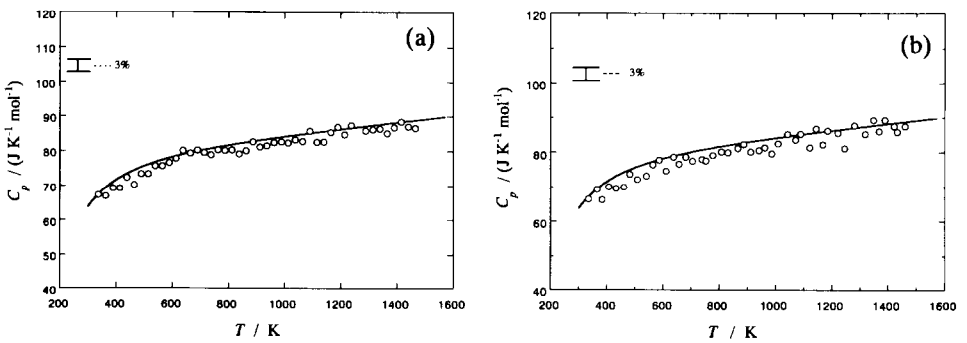

Fig. 11. (a) Heat capacity of UO_2 by the enthalpy method. O, present work; ——, Fredrickson and Chasanov [5]. (b) Heat capacity of UO_2 by the scanning method. O, present work; ——, Fredrickson and Chasanov [5].

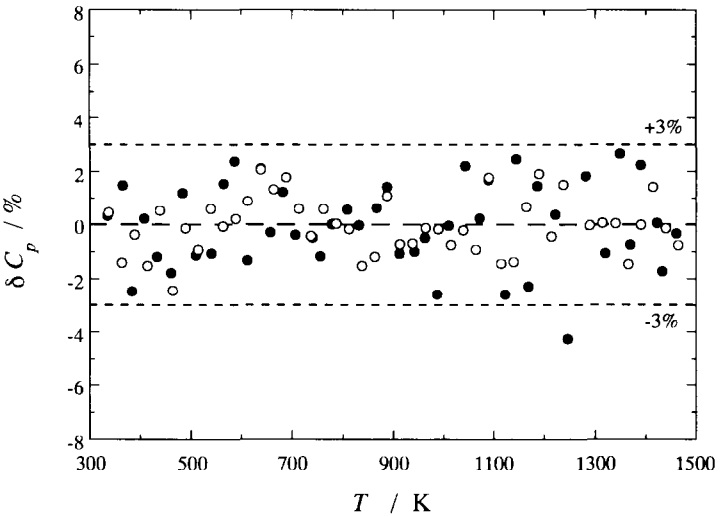

Fig. 12. Deviations of the heat capacity values from the fitting curve for the enthalpy method (○) and the scanning method (●).

the enthalpy method. The deviations of the heat capacity values obtained by both methods from each fitting curve are shown in Fig. 12. The repeatability of the data by the scanning method are slightly worse, by about 0.5–1%, than that by the enthalpy method, particularly above 1000 K. This may be attributable to the temperature gradient in the sample during a scan. However, this problem is not important for measurements by the enthalpy method, because in this case temperature increments are determined from the two temperature measurements, namely the initial and final temperatures, under the condition of a zero scan rate, in which the sample is considered to be in equilibrium. This similarity to adiabatic calorimetry may make the enthalpy method more suitable than the scanning method for a sample of low thermal conductivity.

With the scanning method, it is possible to scan with a single run over the whole temperature range to be measured. Thus, the scanning method has the advantage of reducing the measuring time, while the enthalpy method is rather time-consuming. The choice of the analytical method depends on factors such as the accuracy required, the characteristics of the samples, the number of samples to be measured, etc.

Heat capacities of Ni and Ti: the application to the heat capacity anomaly

Heat capacity measurements were also carried out on Ni and Ti, which are examples of materials that have a thermal anomaly.

Nickel is known to show a thermal anomaly caused by a magnetic phase

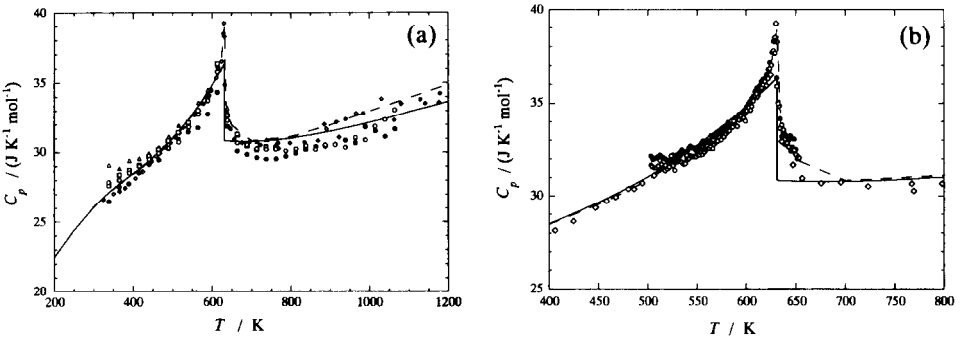

Fig. 13. (a) Heat capacity of Ni by the enthalpy method. △, □, ○, ●, runs 1, 2, 3 and 4 (present work); ——, JANAF data [6]; ◇, TPRC data [7]; – – –, Hultgren et al. [8]. (b) Heat capacity of Ni by the scanning method. ●, ○, runs 1 and 2 (present work); ——, JANAF data [6]; ◇, TPRC data [7]; – – –, Hultgren et al. [8].

transition at 631 K. The results obtained for Ni are shown in Fig. 13(a). Measurements were carried out four times on several samples of different thicknesses. The thickness was 1 mm for the samples of the first and second runs, and 1.5 mm for the third and fourth runs. In the fourth run, the sample and the reference material were interchanged, that is, the Ni sample was placed on the reference side and the α-Al_2O_3 reference material was placed on the sample side.

The four series of data are consistent with each other, within ±3%, and also agree well with literature values [6–8], although out data are slightly lower. This figure shows that even around a thermal anomaly it is possible to determine the heat capacity with a precision of ±3% using this DSC apparatus.

The heat capacity measurements were also carried out by the scanning method, with a long scan over the 473–673 K temperature range. The results are shown in Fig. 13(b). The present values agree well with each other, and are also consistent with the literature values [6–8]. The scanning method has the advantage that it is possible to determine the transition temperature more exactly than the enthalpy method. The transition temperature observed in this study was 629 K.

Titanium is also known to have a thermal anomaly caused by a structural phase transition at around 1160 K. The observed heat capacity values obtained by the enthalpy method are shown in Fig. 14(a). The measurements were carried out twice on the same sample. The two series of data agree very well with each other over the temperature range of the measurements, with a sharp peak at around 1160 K. The present data are lower by 3–7% than the literature values [9, 10] below the transition temperature. This discrepancy may be the effect of some impurities, such as dissolved oxygen. The purities of the samples used in the literature were reported to be 98.7–99.7%, less than that of the sample used here

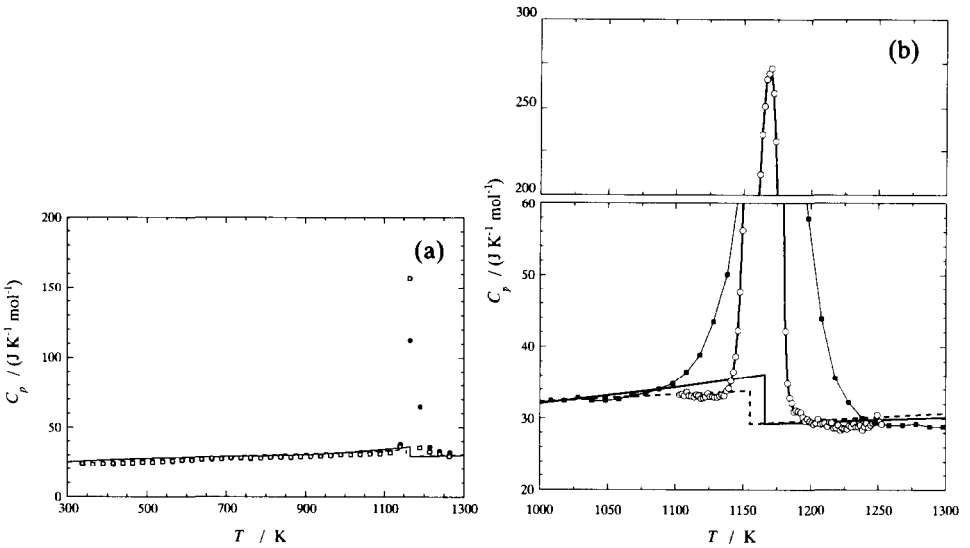

Fig. 14. (a) Heat capacity of Ti by the enthalpy method. □, ●, runs 1 and 2 (present work); ——, JANAF data [6]; – – –, Hultgren et al. [8]. (b) Heat capacity of Ti by the scanning method. ○, present work; ——, JANAF data [6]; – – –, Hultgren et al. [8]; ■, Backhurst [12].

(≥99.9%). Dissolved oxygen in metals has been known to increase the heat capacity [11]. Furthermore, the transition peaks reported in the literature [12] were considerably broader than that of the present result, indicating some effect of impurities. We believe that our heat capacity values are reasonable in this respect. Measurements by the scanning method with a long scan over the 1073–1273 K temperature range showed a sharp peak as shown in Fig. 14(b). The observed transition temperature, which was determined by extrapolating the leading edge of the peak to the baseline, was 1148 K. Although this value is slightly lower than the literature values (1155–1160 K), as can be seen from the pahse diagram of the Ti–O system [13], this disagreement must also be attributable to oxygen impurities in the samples, as mentioned above.

CONCLUSION

A new differential scanning calorimeter (DSC) for heat capacity measurements up to 1500 K has been developed, using a "triple-cell" system and a "triple-adiabatic" temperature control system. The heat capacities of Mo, Pt, UO_2, Ni and Ti were determined from 300 to 1500 K, and the precision of the heat capacity measurements was estimated to be within ±3%. It is concluded that the heat capacity determined by the enthalpy method was more precise than that determined by the scanning method. However, using the scanning method, it is possible to determine

the profile of heat capacity anomalies more exactly then when using the enthalpy method.

ACKNOWLEDGMENTS

We are indebted to Dr. M. Kamimoto and Dr. T. Yoneoka for their discussion and help throughout this work. We also thank Dr. A. Maesono and Sinku-riko Co. for constructing the apparatus with experimental skill. This work was supported financially in part by Monbusho, Japan as a Grant-in-Aid for Developmental Scientific Research, No. 01880025.

REFERENCES

1 B. Wunderlich, J. Therm. Anal., 32 (1987) 1949.
2 R. Hultgren, P.D. Desai, D.T. Hawkins, M. Gleiser, K.K. Kelley and D.D. Wagman, Selected Values of the Thermodynamic Properties of the Elements, Am. Soc. for Metals, Metals Park, OH, 1973, p. 396.
3 H. Yokokawa and Y. Takahashi, J. Chem. Thermodyn., 11 (1979) 411.
4 D.A. Ditmars, A. Cezairliyan and T.B. Douglas, NBS Special Publication, No. 260, 1970, p. 55.
5 D.R. Fredrickson and M.G. Chasanov, J. Chem. Thermodyn., 12 (1970) 623.
6 JANAF Thermochemical Tables, ACS/AIP/NBS, 3rd edn., 1985, p. 1621.
7 Y.S. Touloukian and E.H. Buyco, Thermophysical Properties of Matter, Specific Heat; Metallic Elements and Alloys, IFI/Plenum, New York, 1970, p. 146.
8 R. Hultgren, P.D. Desai, D.T. Hawkins, M. Gleiser, K.K. Kelley and D.D. Wagman, Selected Values of the Thermodynamic Properties of the Elements, Am. Soc. for Metals, Metals Park, OH, 1973, p. 350.
9 JANAF Thermochemical Tables, ACS/AIP/NBS, 3rd edn., 1985, p. 1818.
10 R. Hultgren, P.D. Desai, D.T. Hawkins, M. Gleiser, K.K. Kelley and D.D. Wagman, Selected Values of the Thermodynamic Properties of the Elements, Am. Soc. for Metals, Metals Park, OH, 1973, p. 516.
11 J. Nakamura, Y. Takahashi, S. Izumi an M. Kanno, J. Nucl. Mater., 88 (1980) 64.
12 I. Backhurst, J. Iron Steel Inst. (London), 189 (1958) 124.
13 J.L. Murray and H.A. Wriedt, Bulletin of Alloy Phase Diagrams, 8(2) (1987) 148.